Earth, Planets and Space
a SpringerOpen Journal

FULL PAPER

Open Access

CrossMark

Descent of tremor source locations before the 2014 phreatic eruption of Ontake volcano, Japan

Masashi Ogiso[1*], Hirotoshi Matsubayashi[2] and Tetsuya Yamamoto[1]

Abstract

On 27 September 2014, Ontake volcano, in central Japan, suddenly erupted without precursory activity. We estimated and tracked the source locations of volcanic tremor associated with the eruption at high temporal resolution, using a method based on the spatial distribution of tremor amplitudes. Although the tremor source locations were not well constrained in depth, their epicenters were well located beneath the erupted crater and the summit. Tremor sources were seen to descend approximately 2 km over a period of several minutes prior to the beginning of the eruption. Detailed analysis of the time series of tremor amplitudes suggests that this descent is a robust feature. Our finding may be an important constraint for modeling the 2014 eruption of Ontake volcano as well as for monitoring activities on this and other volcanoes.

Keywords: Tremor location, Migration, Mechanism of phreatic eruption, Volcano monitoring, Ontake volcano

Background

Ontake volcano, in central Japan, is the nation's second highest volcano with an elevation of 3067 m. According to the Japan Meteorological Agency and the Volcanological Society of Japan (2013), magmatic eruptions have occurred four times at Ontake during the last 100,000 years in addition to occasional phreatic eruptions. Only three eruptions were recorded in human history before the 2014 eruption. The first eruption occurred in the early morning of 28 October 1979 when there were only two seismic stations around Ontake, one located on 12 km north and the other on 13 km southeast. Although hypocenter determination of its associate earthquakes was impossible at that time, these two stations recorded precursory seismicity that started in the previous evening (Aoki et al. 1980). Approximately 200,000 tonnes of ash was produced during the 1979 eruption (Kobayashi 1980). The second eruption occurred on the middle of May, 1991. Aerial photographs by the press detected fumarolic activity from one of the craters formed during the 1979 eruption. Ash was distributed in the area of about 200 m long by 100 m width just in the

east of the craters. The amount of ash was not more than dozens of tonnes. On-site survey estimated that the eruption occurred between 13 and 18 May. Preceding the eruption, seismicity at Ontake had increased since late April and many tremors were observed at the same time (Matsumoto Weather Station 1991; Nagoya University 1991). The third eruption occurred in 2007. Volcanic earthquake swarm began on the end of December 2006 (Otsuka and Fujimatsu 2009). On 25 January, the largest volcanic tremor during the 2007 activity occurred. This tremor contains a component of very long period (about 20–100 s) (Nakamichi et al. 2009). At almost the same time of the beginning of volcanic earthquake swarm, inflation of the volcanic edifice was detected by continuous GPS observations (Takagi et al. 2007). Although significant precursors were observed in both seismicity and crustal deformation, the 2007 eruption was only recognized afterward when ash was seen on top of snow during an on-site survey. The ash was too little to estimate its amount. The date of the eruption was not specified in the 2007 activity (Japan Meteorological Agency 2008).

The Tokyo Volcano Observation and Information Center, Japan Meteorological Agency (hereafter Tokyo VOIC) monitors active volcanoes in the Kanto and Chubu regions of Japan, including Ontake, using seismic data, ground

* Correspondence: mogiso@mri-jma.go.jp
[1]Meteorological Research Institute, Japan Meteorological Agency, 1-1 Nagamine, Tsukuba, Ibaraki 305-0052, Japan
Full list of author information is available at the end of the article

Springer

Ogiso *et al. Earth, Planets and Space* (2015) 67:206

Page 2 of 12

deformation measurements, video observations, and on-site surveys. Around 11:52 on 27 September 2014 (dates and times are Japan Standard Time, 9 h ahead of UTC), an eruption suddenly began, causing pyroclastic flows that were recorded by a video camera placed on the southern flank of Ontake (Tokyo Volcano Observation and Information Center 2014). Clouds obstructed any views of active craters from video observations at that time, but new craters were later identified by aerial observations (e.g., Kaneko et al. 2014). Kaneko et al. (2014) also reported that the impact craters of volcanic bombs were distributed mainly in the northeast of erupted craters by careful analysis of aerial photographs. The density of volcanic bombs was extremely high (more than 10 craters per 16 m^2) within 500 m from craters. Volcanic bombs were not found over 1 km away from the erupted craters in the photographs. Diameters of the impact craters were between 10 cm and 1 m. The type of eruptions was determined to be phreatic, and the amount of ashfall was estimated to be about 600,000 to 1,500,000 tonnes (Takarada et al. 2014). According to the official report from Tokyo Volcano Observation and Information Center (2014), the eruption continued until at least 10 October. Because 27 September was a holiday and the weather was fine in this area, there were many hikers near the summit when the eruption began. As a result, there were 57 confirmed fatalities and 6 people remain missing (Nagano Prefectural Government 2015). This eruptive event left us many issues in not only volcanological but also social aspects. Even if an eruption is small and there are no casualties, the eruptive event sometimes leaves a large social impact, leading to difficult challenges of scientific communication (e.g., Leonard et al. 2014). Similar to the case of Tongariro volcano (Leonard et al. 2014), the 2014 eruption of Ontake volcano revealed some challenges to the mitigation of volcanic disaster, and many

investigations have been conducted by both national and local governments (Yamaoka 2015).

On 10 and 11 September, 17 days before the 2014 eruption, the level of seismicity beneath Ontake volcano suddenly increased and then gradually decreased (Fig. 1). However, unlike the case in 2007, no significant ground deformations, volcanic tremor nor unusual very long period earthquakes were observed in 2014 until just before the eruption. The first volcanic tremor was observed at 11:41 on 27 September, only 11 min before the eruption. Ground deformation suggesting the inflation of volcanic edifice was recorded by a tiltmeter at almost the same time as the tremor began (e.g., Takagi et al. 2014), and it turned out the deflation on 11:52, the same time as the eruption.

Observations of the volcanic tremor and ground deformation at Ontake before the 2014 eruption contain some important information about eruption-related activities. In this paper, we report estimates of the source locations of volcanic tremor at the time of the eruption and discuss what this information reveals its volcanic processes prior to the eruption.

Data and methods

Tokyo VOIC monitors volcanic seismicity at Ontake in cooperation with Nagoya University, the National Research Institute for Earth Science and Disaster Prevention, the Nagano Prefectural Government, and the Gifu Prefectural Government. In this study, we used data from five seismometers around Ontake (Fig. 2). A broadband seismometer (natural period of 30 s) operated at station ROPW, and short-period (1 s) seismometer operated at the others. Seismic records were digitized in sampling frequency of 100 Hz with 24-bit resolution at each station.

The seismic records from the five stations (vertical component) from 11:40 to 12:20 on 27 September are
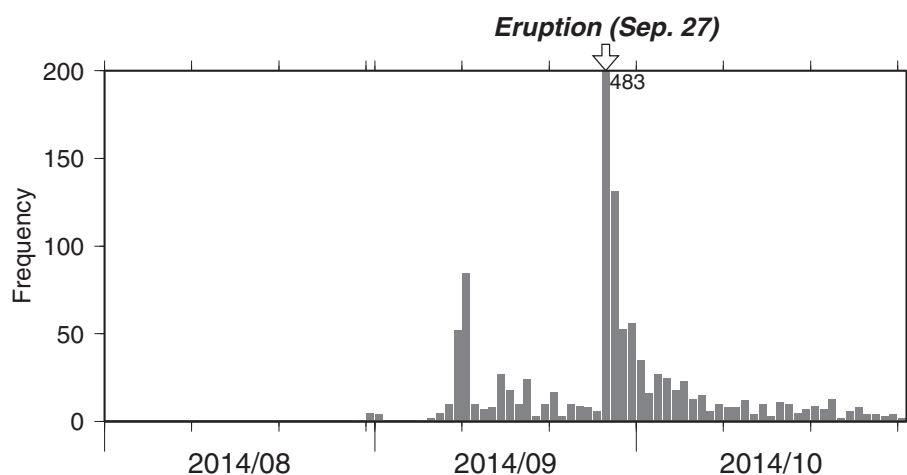

Fig. 1 Daily frequency of volcanic earthquakes on Ontake volcano from August through October 2014 (Tokyo VOIC data). The number of earthquakes on 27 September is 483, which is off scale in the figure
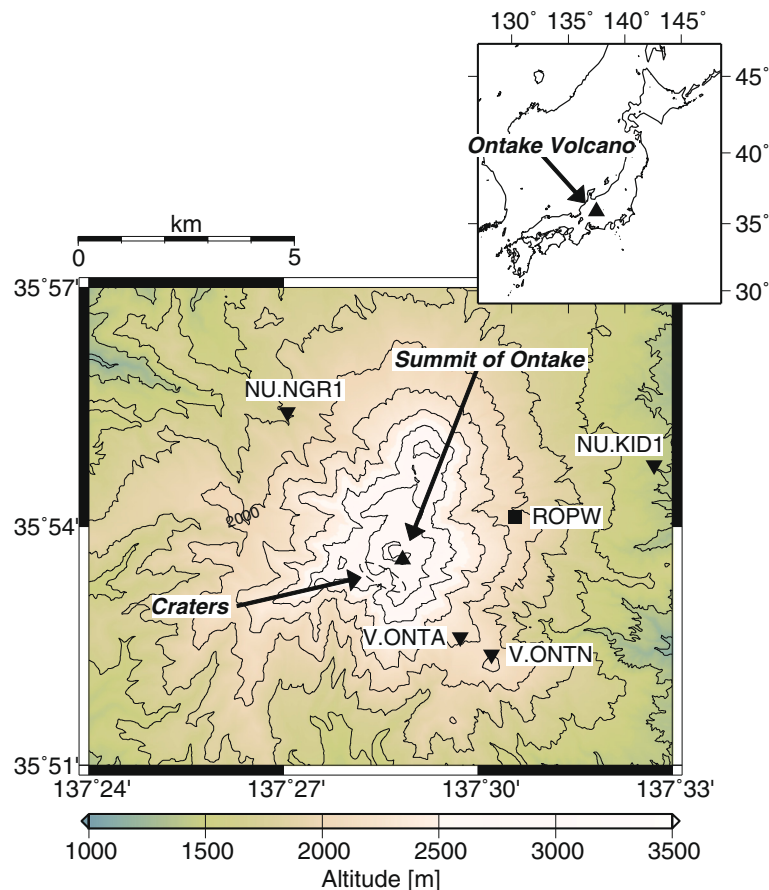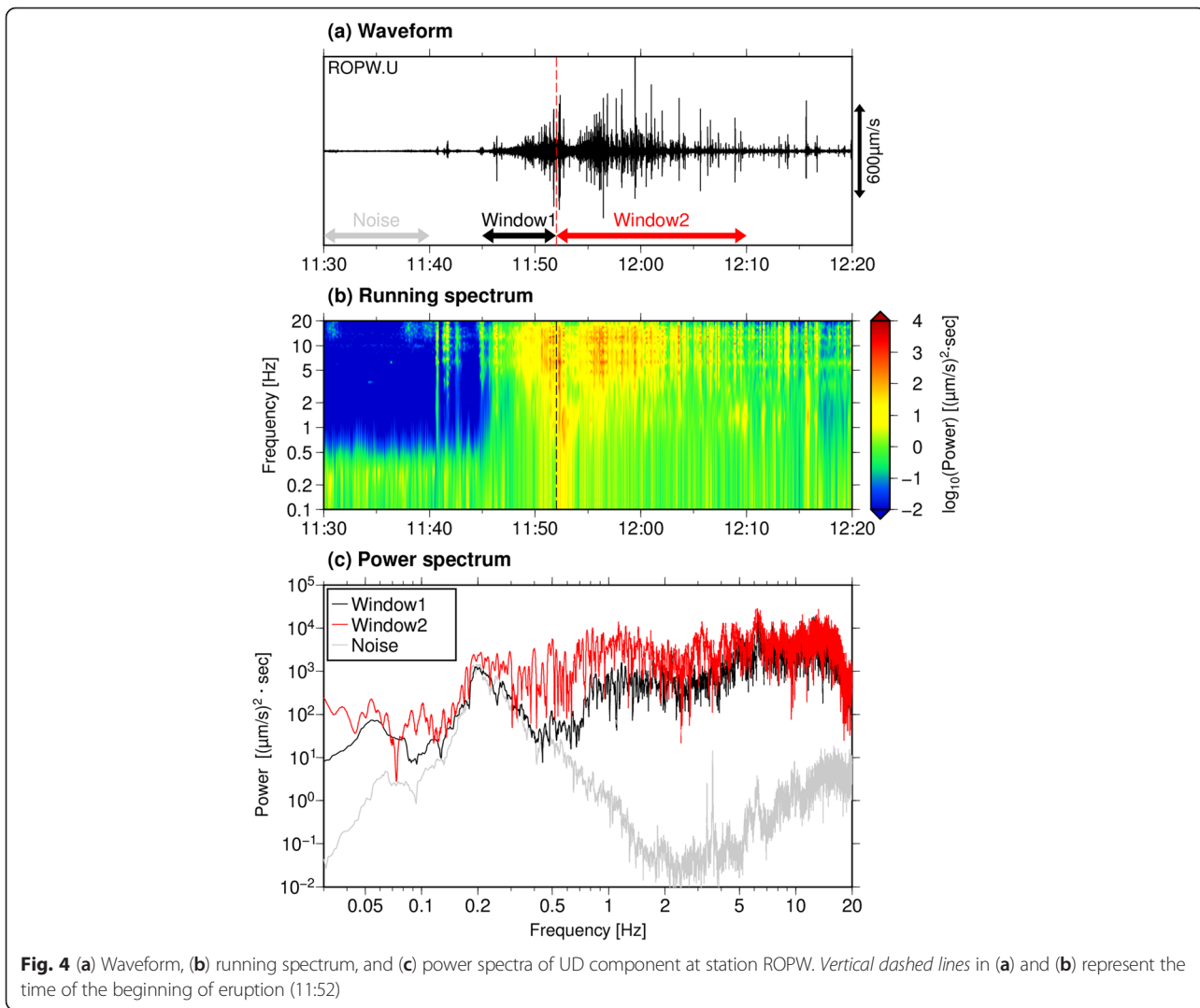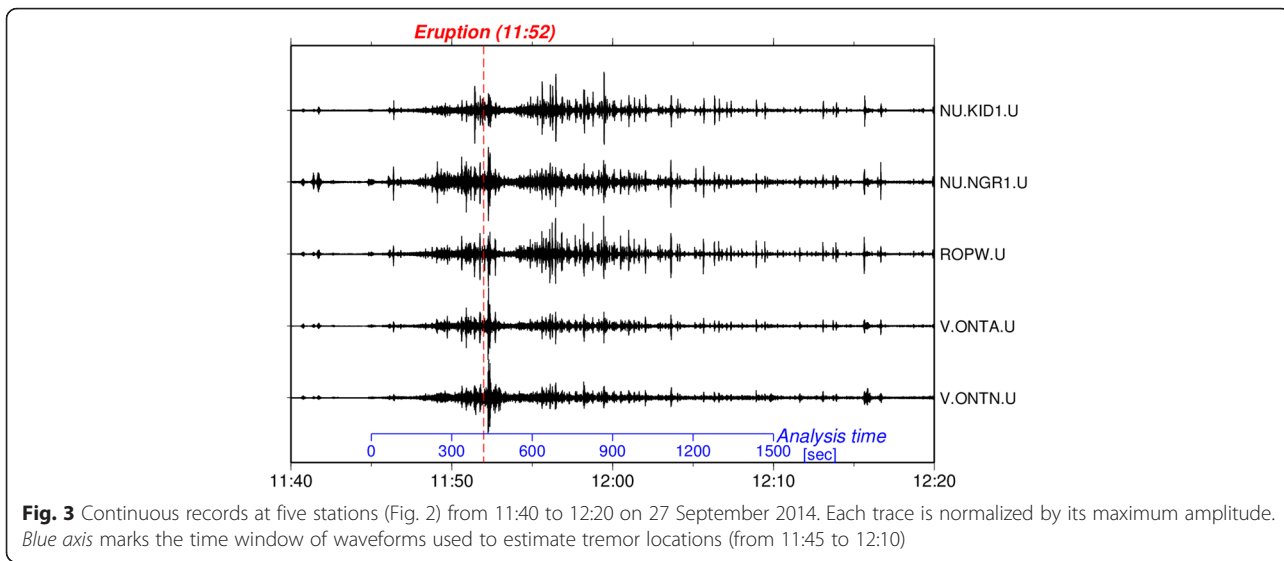
Ogiso *et al. Earth, Planets and Space* (2015) 67:206

Page 3 of 12

Fig. 2 Map of the study area (location in *inset*) showing topography and the distribution of seismic stations used in this study around Ontake volcano. Contour interval is 200 m. A broadband (30 s) seismometer operated at station ROPW (*square*) while short-period (1 s) seismometers operated at the other stations (*inverted triangles*). Approximate location of the erupted craters on 27 September 2014 was determined by aerial survey after the eruption (Kaneko et al., 2014)

shown in Fig. 3. Intermittent tremor is first recognized at 11:41 and becomes continuous about 11:45. Continuous tremor ended on 1 October (Tokyo Volcano Observation and Information Center 2014). We focus on the tremor just before and after the eruption began at 11:52. We estimated locations of the tremor in the 1500-s time window from 11:45 to 12:10, a period when continuous tremor was apparent on all local network stations. We show a running spectrum and power spectra at station ROPW in Fig. 4. We calculated running spectrum using an autoregressive model with 10.24-s time window, sliding by every 5.12 s. Power spectra were calculated in the following three time windows; noise (before tremor), window 1 (before eruption), and window 2 (after eruption). We can recognize the beginning of continuous tremor around 11:45 from its running spectrum (Fig. 4b). Figure 4c shows that the volcanic tremor is rich in power above 0.5 Hz at both windows 1 and 2, while the powers of tremor and noise are almost the same around the

frequency of 0.2 Hz. There is an interesting feature that the powers of tremor on both windows 1 and 2 under 0.1 Hz are stronger than those of noise. This feature may relate to the tilt signals recorded at this station (Takagi et al. 2014).

Usually, a tremor has no clear onsets of P or S waves; thus, the conventional method of source location using phase arrival times is not applicable. We adopted the amplitude source location (ASL) method, which utilizes the spatial distribution of tremor amplitude (Yamasato 1997, Jolly et al. 2002, Battaglia and Aki 2003, Kumagai et al. 2010). One of the advantages of the ASL is high temporal resolution, making it possible to follow the migration of sources during a tremor sequence (Kumagai et al. 2011, Ogiso and Yomogida 2012).

The ASL method has been summarized by Kumagai et al. (2010). The seismic amplitude of body waves of frequency f at station i, $A_i(f)$, can be represented as

Ogiso *et al. Earth, Planets and Space* (2015) 67:206

Page 4 of 12

Fig. 3 Continuous records at five stations (Fig. 2) from 11:40 to 12:20 on 27 September 2014. Each trace is normalized by its maximum amplitude. *Blue axis* marks the time window of waveforms used to estimate tremor locations (from 11:45 to 12:10)

Fig. 4 (**a**) Waveform, (**b**) running spectrum, and (**c**) power spectra of UD component at station ROPW. *Vertical dashed lines* in (**a**) and (**b**) represent the time of the beginning of eruption (11:52)

Ogiso *et al. Earth, Planets and Space* (2015) 67:206

Page 5 of 12

$$A_i(f) = A(f) \cdot \exp(-Br_i)/r_i \cdot S_i(f), \qquad (1)$$

where $A(f)$ is the source amplitude, r_i is the distance from the source to the station i, $S_i(f)$ is the site amplification factor at ith station, and B encompasses the quality factor Q and the average velocity of the medium β such that

$$B = \pi f / Q\beta. \qquad (2)$$

We explain the estimation of the site amplification factor, $S_i(f)$, later. If we assume the source location, the source amplitude $A(f)$ can be calculated from the observed amplitudes at a total of N stations:

$$A(f) = \frac{1}{N} \sum_{i=1}^{N} \{A_i(f)/S_i(f)\} \cdot r_i \exp(Br_i). \qquad (3)$$

In this study, we assumed that the source amplitude $A(f)$ depends only on frequency, although $A(f)$ also depends on the azimuthal relationship between the source and station due to the inhomogeneous radiation patterns of seismic source. However, Takemura et al. (2009) showed that scattering due to small-scale heterogeneity in the crust masks the radiation pattern at frequencies higher than 5 Hz. Taking the relatively strong crustal heterogeneities in volcanic areas (e.g., Yamamoto and Sato 2010) into consideration, our assumption that source amplitudes have no azimuthal dependency is reasonable for frequencies higher than 5 Hz. In this study, we used 5–10 Hz filtered waveforms to satisfy this assumption. Signal-to-noise ratio of 5–10 Hz was high to be reliable location estimation (Fig. 4).

To evaluate the validity of the source location, we define normalized residual by the following approximation:

$$\text{residual} \equiv \frac{\sum_{i=1}^{N} \{A_i(f)/S_i(f) - A(f) \exp(-Br_i)/r_i\}^2}{\sum_{i=1}^{N} \{A_i(f)/S_i(f)\}^2}. \qquad (4)$$

We conducted a grid search in the whole area of Fig. 2 with an interval of 0.001° in both latitudinal and longitudinal directions and 0.1 km in the depth direction to find the grid cell with the minimum residual. We used the root-mean-square (RMS) amplitude in a given time window as the observed amplitude $A_i(f)$ at each station. This study used the frequency range of 5–10 Hz for

RMS amplitude calculations; hence, the frequency f is 7.5 Hz in our equations. We assumed that the observed waveforms at each station were composed of direct S waves in this frequency range and thus adopted 2.31 km/s for the velocity of the medium, which is the S wave velocity that Tokyo VOIC uses for hypocenter determination at Ontake volcano. This velocity was estimated from the seismic-refraction profile derived by Ikami et al. (1986) with some trial-and-error modifications (Koji Kato, personal communication). Because the attenuation structure of Ontake is unclear, we assumed Q to be constant at 50, a commonly used approximation in volcanic areas (Koyanagi et al. 1995, Battaglia and Aki 2003, Ogiso and Yomogida 2012, Kumagai et al. 2013). We used only the vertical component waveform of each station.

Site amplification factors play an important role in the ASL method (Kumagai et al. 2013). We evaluated them for each station by using the coda normalization method, based on the RMS amplitude ratio of coda waves (Phillips and Aki 1986). To estimate the site amplification factors, we used the records of nine earthquakes that occurred far from Ontake (Fig. 5). We selected five time windows of 10 s, successively shifted by 5 s, that started at a time before the earthquake representing twice the travel time of the direct S wave. We calculated RMS amplitudes in each time window from the 5–10 Hz band-pass filtered waveform. We defined a noise level for each station using the RMS amplitude of the time period just before the direct P wave arrival, and we accepted only time windows with signal-to-noise ratios larger than 3.0. We then determined the RMS amplitude ratio with respect to the reference station V.ONTN in each time window and averaged the ratios of all the time windows of the nine earthquakes using a common logarithmic scale. We also calculated a standard deviation of the ratio at each station. The resulting site amplification factors of the five stations and their standard deviations are listed in Table 1. Stations NU.NGR1 and ROPW had fewer data points than the other stations, because NU.NGR1 had more local noise and because ROPW was offline before 19 September. Stations V.ONTN, NU.KID1, and ROPW show large amplification factors (larger than 5). Subsurface structure and topography affect amplification factors, resulting in up to 100 times larger than seismic basement in some stations (e.g., Kawase and Matsuo 2004). We only point out that further investigations will be required to confirm the reasons of such a large site amplification factors in those three stations, although it is out of our main purpose in this paper. We used the values listed in Table 1 for correcting site amplifications as we determined tremor amplitudes.
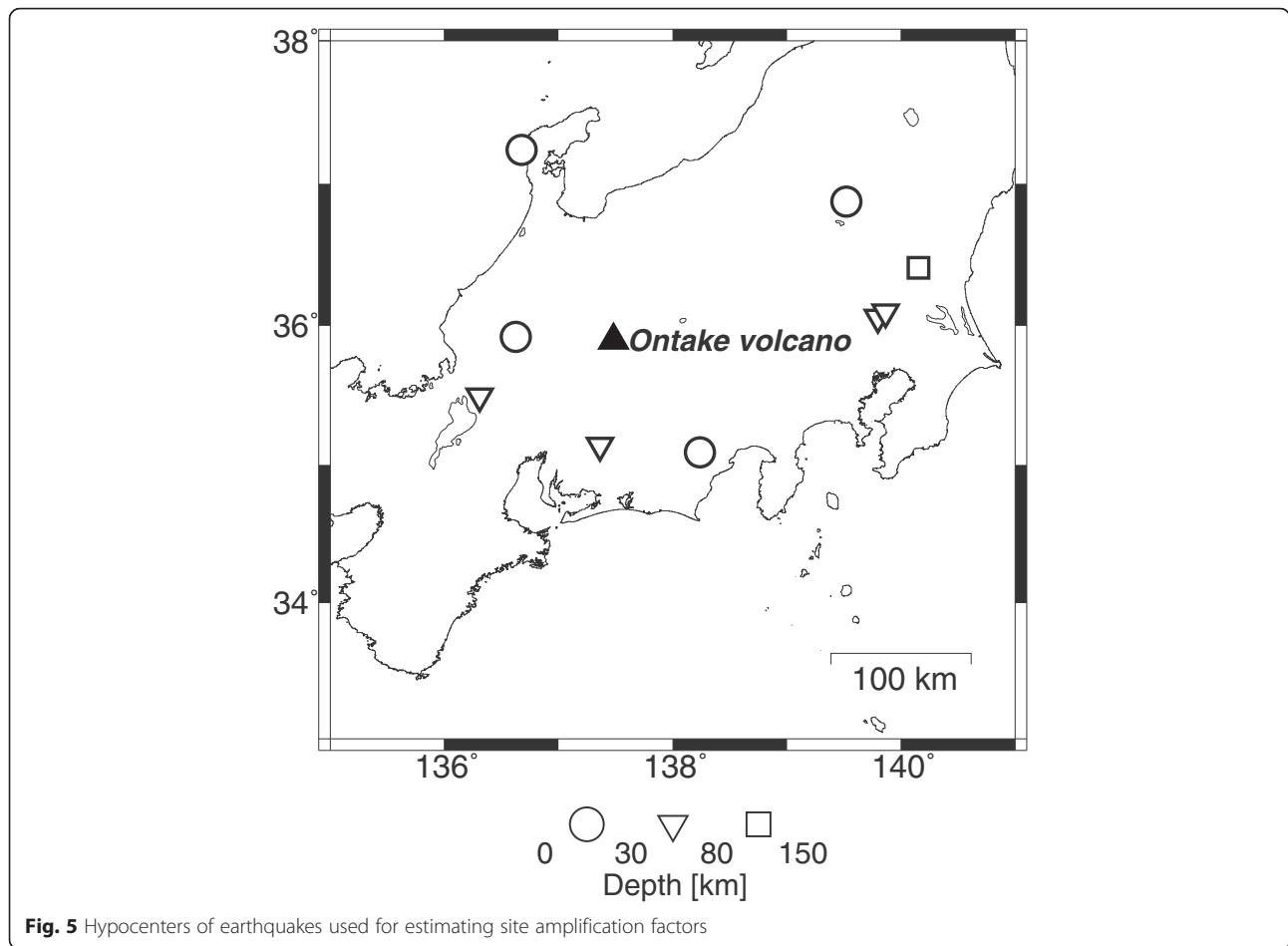
Ogiso *et al. Earth, Planets and Space* (2015) 67:206

Page 6 of 12

Fig. 5 Hypocenters of earthquakes used for estimating site amplification factors

Results
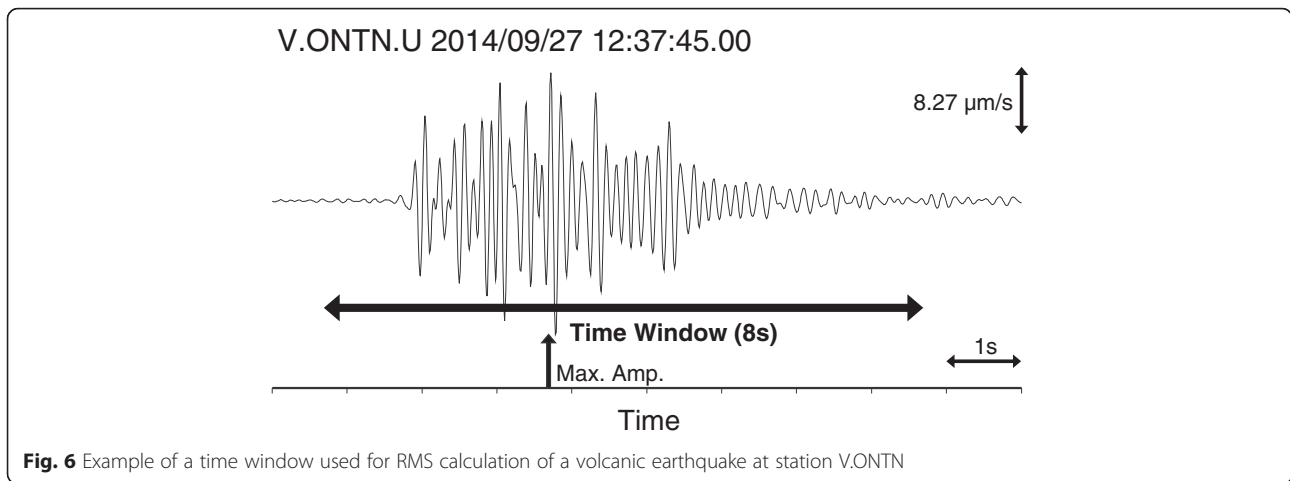
Source locations of volcanic earthquakes

As a check of the ASL method, we compared locations of volcano tectonic earthquakes at Ontake estimated by the ASL with the locations estimated from phase arrivals of P and S waves by Tokyo VOIC. Earthquakes were selected from continuous records of 27 September, and an 8-s time window was chosen, starting at 3 s before the maximum amplitude was observed in the 5–10 Hz

filtered waveform (Fig. 6). This time window was almost equal to the duration time of a typical volcano tectonic earthquake in this area. To estimate an error of the ASL method, we added random fluctuations to the site amplification factor of each station based on the assumption that the site amplification factor follows a log-normal distribution (standard deviations are listed in Table 1), then we conducted a grid search 100 times for each event with the fluctuated site amplification factors. We defined an error as a standard deviation in each axis (longitudinal, latitudinal, and depth). Location errors by the ASL were roughly ± 2 km in the longitudinal and depth directions and ± 1 km in the latitudinal direction.

Figure 7 shows the locations estimated by ASL and taken from the Tokyo VOIC catalogue for common events. Hypocenters by ASL has a spread of 4 km in the longitudinal and depth directions and 2 km in the latitudinal direction, which is almost equal to the scale of location errors mentioned above, while those of Tokyo VOIC catalogue also have a spread of about 2 km in latitudinal and depth directions and 1 km in longitudinal

Table 1 Site amplification of seismic stations on Ontake with respect to station V.ONTN, based on the configuration of seismometers and data loggers on 27 September 2014

Station	Amplification factor	Standard deviation (log scale)	Number of data
NU.KID1	6.0223	0.1027	35
NU.NGR1	1.6722	0.1071	16
ROPW	12.4295	0.1085	15
V.ONTA	5.3282	0.0562	35
V.ONTN	1.0	(none)	(none)

Ogiso *et al. Earth, Planets and Space* (2015) 67:206

Page 7 of 12

Fig. 6 Example of a time window used for RMS calculation of a volcanic earthquake at station V.ONTN

direction. These spreads are caused by probabilistic errors in site amplification factors for the ASL case and by the phase reading accuracy for the Tokyo VOIC catalogue. In addition, the comparison of Fig. 7 shows that a centroid of hypocenters calculated by the ASL was systematically shallower and to the east to that of Tokyo VOIC catalogue. We attribute this difference to the limitation of the station distribution we used (Fig. 2). The presence of volcanic tremor in the analyzed records on 27 September might also cause this systematic difference. Because the ASL method assumes a point source when estimating locations, waves from two or more simultaneous sources may affect the estimation by the ASL.

Source locations of volcanic tremor

In estimating the source locations of tremor, we adopted a time window of 30 s for assessing RMS amplitude at each station and shifted the window by 15-s increments from 11:45 to 12:10 on 27 September. The beginning of the time window was set for each station to accommodate its travel time from the assumed tremor source (Kumagai et al. 2010). The definition and calculation of error bars are the same as for the earthquake location explained in the previous section.

Figure 8 shows the result of tremor location estimations. In this analysis, we assumed that wave trains of tremor consisted of body waves or S waves in Eq. 1. For comparison, we also estimated the tremor location with
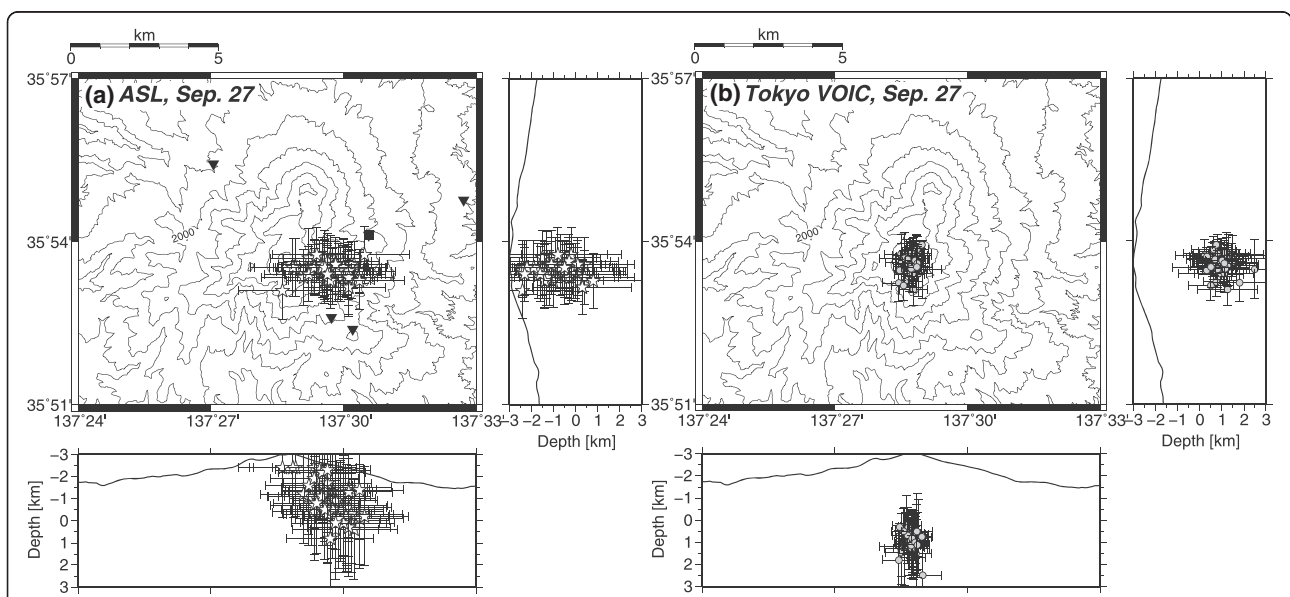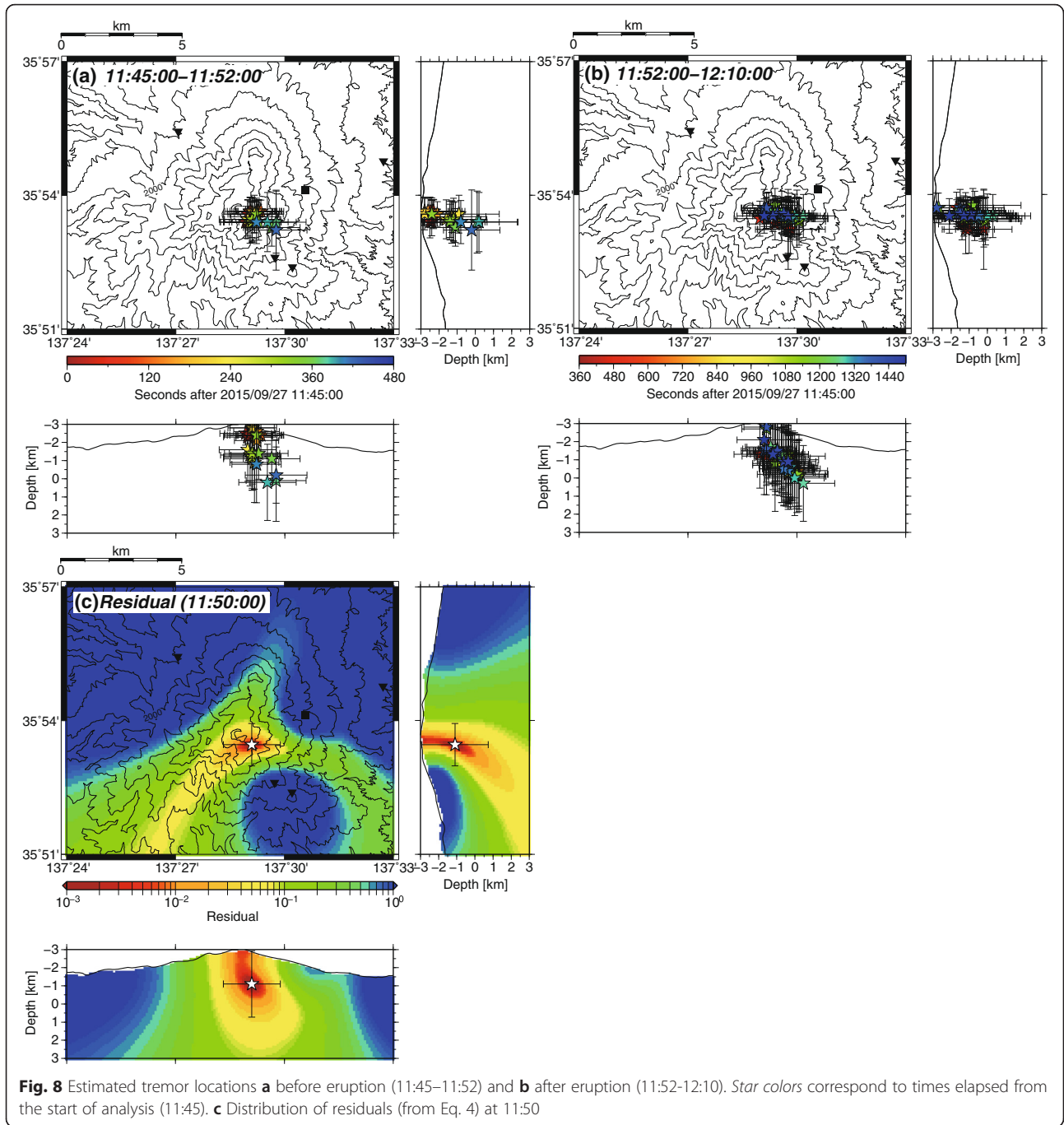

Fig. 7 Hypocenters of volcano-tectonic earthquakes on September 27 determined by **a** the ASL method and **b** routinely determined by Tokyo VOIC. *Error bar* of each event was numerically estimated (see text) for (**a**) and ± standard error for (**b**)

Ogiso *et al. Earth, Planets and Space* (2015) 67:206

Page 8 of 12

Fig. 8 Estimated tremor locations **a** before eruption (11:45–11:52) and **b** after eruption (11:52-12:10). *Star colors* correspond to times elapsed from the start of analysis (11:45). **c** Distribution of residuals (from Eq. 4) at 11:50

the assumption of dominant surface waves in tremor. Small residuals in the assumption of body waves show that the whole wave trains of tremor consisted mainly of body waves (see Appendix). A plot of residuals shows that horizontal locations were well constrained compared with the depths (Fig. 8c). The epicenters of tremor were located in the summit area, extending from about 2 km above sea level to 0.5 km below sea level, both before and after the eruption (Fig. 8a, b). Epicenters appear

to have drifted to the east with increasing depth. This feature is similar to the case of earthquake locations (Fig. 7). Taking into account the systematic estimation bias of the ASL method discussed in the previous section, tremor locations may actually have been in the southwest of the summit beneath the craters (see Fig. 2) and deeper than our estimate.

Figure 8a shows that the tremor source locations systematically descended before the eruption. This apparent

Ogiso *et al. Earth, Planets and Space* (2015) 67:206

Page 9 of 12

descent should not be caused by the change of wave excitation transition from body to surface waves in the tremor sequence. Instead, this feature may be partly explained by random errors in the site amplification factors. To evaluate this possibility, we compared the sequence of tremor depths to the time series of the observed amplitudes at each station, normalized with respect to V.ONTA, the nearest station to the craters (Fig. 9). We also calculated a range of amplitude ratios at each station from the standard deviation of its site amplification factor (Table 1), which was indicated by the length of bars in Fig. 9. Taisne et al. (2011) successfully tracked the migration of volcanic tremor from deep to shallow in depth with a similar approach using tremor amplitude ratios. Different from Taisne et al. (2011), the depth of tremor locations in this study increased steadily, starting at around 120 s (11:47), until the time of the eruption at 420 s (11:52). Tremor amplitudes at stations V.ONTN and ROPW increased before the beginning of the eruption and remained fairly

constant afterwards. It is particularly difficult to interpret that amplitude variations at V.ONTN were caused by random errors in its site amplification factor. Given the locations of these two stations and V.ONTA (Fig. 2), these systematic changes in amplitude are consistent with changes in source depth. Although the amplitude ratios of each station had some variations, we conclude that the descent of tremor sources prior to the eruption was not an artifact but an actual feature. The rate of descent is highly uncertain at this time because of the lack of depth accuracy in the ASL estimates (Figs. 7 and 8).

Possible model for descending tremor source locations

Because the ASL method assumes a point source for seismic events, we can interpret the descent of tremor sources in two ways: (a) there is a point source of tremor that moved downwards, or (b) there is a finite source area of tremor, and the descent indicates the migration of the portion of the area that was generating strong
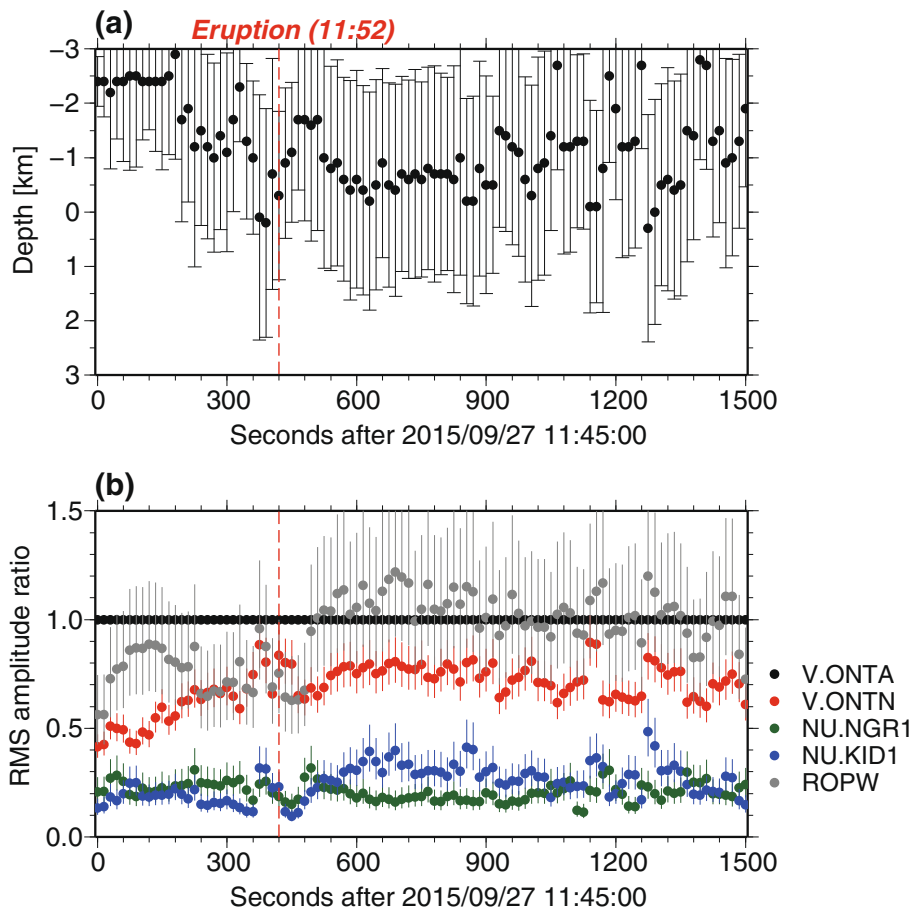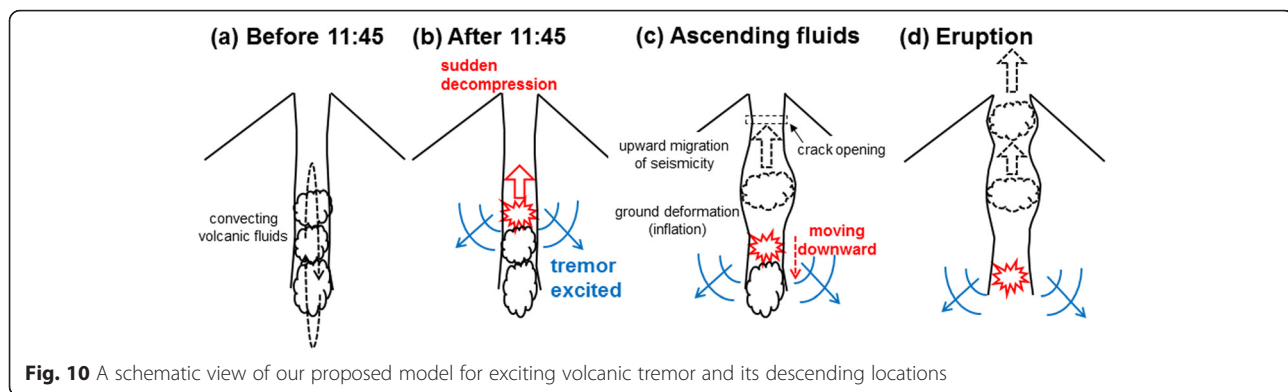

Fig. 9 Time sequences of (**a**) tremor depth and (**b**) RMS amplitude ratios with respect to station V.ONTA. *Error bars* of tremor depth were numerically estimated, and RMS amplitude ratios were calculated by the propagation of site amplification errors.

Ogiso *et al. Earth, Planets and Space* (2015) 67:206

Page 10 of 12

Fig. 10 A schematic view of our proposed model for exciting volcanic tremor and its descending locations

motion. In this section, we propose a point-source model based on the first interpretation.

We consider it natural to assume the presence of a well-developed hydrothermal system beneath Ontake. Nakamichi et al. (2009) interpreted the source processes of a very long period event prior to the 2007 eruption as the response of a shallow hydrothermal system to the heat supplied by intruding magma. In the scenario we envision, mixture of volcanic gases and liquid water is convecting in a hydrothermal conduit (Fig. 10a). Masses of the fluid mixture might be formed in gaps of preexisting faults or cracks in the conduit and large stress gradient corresponding to the distribution of the masses are likely to exist in the conduit. At approximately 11:45 on 27 September, a sudden decompression event commenced at a shallow depth (Fig. 10b). Although any minor fumarolic activity around the eruption site may have occurred in response, no video observations or witnesses recorded it. The decompression induces phase transition of the volcanic fluids with exciting volcanic tremor, leading it to flash into a gaseous phase. These disturbances propagate downwards in the hydrothermal system. At the same time, ascending volcanic gases and water vapor open a crack just beneath the eruption crater (Maeda et al. 2015), together with upward migration of seismicity (Kato et al. 2015) (Fig. 10c). The ascending gases cause the ground inflation detected by tiltmeter (Takagi et al. 2014). Although the ascending gases might generate volcanic tremor simultaneously with descending sources, they may not be detected in our analysis because we assumed a point source in the ASL method (Eq. 1). The inferred descent of tremor locations just before the eruption is a key factor in our interpretation of the phreatic eruption process at Ontake.

Our findings may have further implications for monitoring volcanic activities. Because the ASL method can be applied in near-real time, it may

enable us to detect and track the migration of volcanic tremor sources immediately after the beginning of tremor is recognized. Although its mechanism is not yet known, migration of tremor source locations may be a distinctive precursor of phreatic eruptions in general. Thus, early recognition of tremor source locations and their migration may afford an early warning of any future phreatic eruptions at Ontake and other active volcanoes.

Conclusions

We used the ASL method to estimate the source locations of volcanic tremor with high temporal resolution just before and after the 27 September 2014 phreatic eruption of Ontake volcano. Our result showed that the tremor source was located beneath the eruption craters and the summit. This source steadily descended during the period of several minutes just before the beginning of the eruption. Although the precision of absolute locations was limited (especially for depths) owing to the accuracy of site amplification factors and insufficient station distribution, our careful check of the observed amplitude ratios of the tremor data suggests that our finding of a descending source is robust.

We hypothesize that the tremor was excited by the decompression of volcanic fluids that took place on a downward-propagating front. At the same time, ascending volcanic gases caused the inflation of the summit area of Ontake, opened a crack just beneath the craters together with active seismicity, and finally escaped in a phreatic eruption. Descending tremor source locations should be further investigated as an immediate precursor of phreatic eruptions and for possible use in monitoring volcanic activities.

Appendix

We assumed that S waves are dominant in the frequency range of 5–10 Hz in tremor records. Here, we show the

Ogiso *et al. Earth, Planets and Space* (2015) 67:206
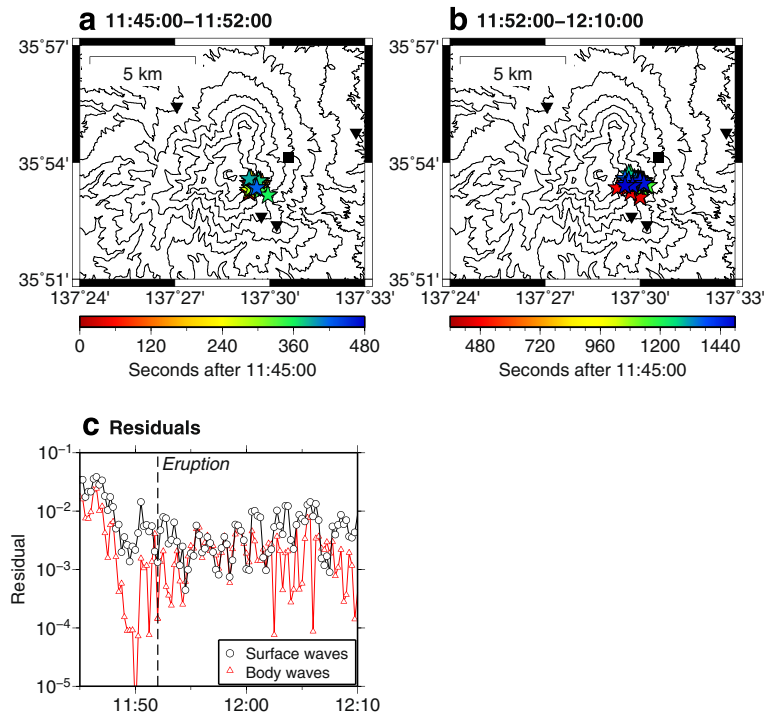
Page 11 of 12

Fig. 11 Epicentral locations of volcanic tremor at **a** 11:45–11:52 and **b** 11:52–12:10 and **c** temporal variations of residuals for the case of surface wave assumption

result of another case that surface waves are dominant. In such a case, Eq. 1 is replaced by

$$A_i(f) = A(f) \cdot \exp(-Br_i)/\sqrt{r_i} \cdot S_i(f). \tag{A1}$$

We conducted the grid search in the same condition except that the assumed sources were restricted on the surface and 2.13 km/s for the medium velocity β. Figure 11 shows the results. Hypocenters are estimated slightly in the east of the erupted craters. Residuals (Fig. 11b) are larger than the case of S waves in every time that we analyzed. This result strongly suggests the body waves are dominant in the whole wave trains of tremor which we analyzed so that excited waves should not change from body to surface waves.

Competing interests
The authors declare that they have no competing interests.

Authors' contributions
MO conducted the waveform analyses and drafted the manuscript. HM and TY proposed and refined the hypothesis of location migration and revised the manuscript. All authors read and approved the final manuscript.

Acknowledgements
We thank the staff of Nagoya University and the Nagano Prefectural Government for their permission to use seismic waveforms and for their efforts to maintain their seismic stations. Koji Kato kindly helped us to collect seismic waveforms and advised us the velocity structure around Ontake volcano. Yoshiro Masuda and Yutaka Nagaoka also helped us to collect

Author details
[1]Meteorological Research Institute, Japan Meteorological Agency, 1-1 Nagamine, Tsukuba, Ibaraki 305-0052, Japan. [2]Anet Co., 2-23 Kanda-Sudacho, Chiyoda-ku, Tokyo 101-0041, Japan.

References
Aoki H, Oida T, Fujii I, Yamazaki F (1980) Seismological study of the 1979 eruption of Ontake Volcano. In: Aoki H (ed) Investigation of volcanic activity and disasters caused by the 1979 eruption of Ontake volcano. Nagoya University, Nagoya, pp 55–74 (In Japanese)
Battaglia J, Aki K (2003) Location of seismic events and eruptive fissures on the Piton de la Fournaise volcano using seismic amplitudes. J Geophys Res 108(B8):2364. doi:10.1029/2002JB002193
Ikami A, Yoshii T, Kubota S, Sasaki Y, Hasemi A, Moriya T, Miyamachi H, Segawa-Matsu'ura R, Wada K (1986) A seismic-refraction profile in and around Nagano prefecture, central Japan. J Phys Earth 34:457–474. doi:10.4294/jpe1952.34.457
Japan Meteorological Agency (2008) Volcanic activity of Ontakesan (from March 2007 to June 2007). Report of Coordinating Committee for Prediction of Volcanic Eruption 97:14–29 (In Japanese)
Japan Meteorological Agency and the Volcanological Society of Japan (2013), Ontake, in National catalogue of the active volcanoes in Japan. (fourth edition,

Ogiso *et al. Earth, Planets and Space* (2015) 67:206

Page 12 of 12

English version), http://www.data.jma.go.jp/svd/vois/data/tokyo/STOCK/souran_eng/volcanoes/053_ontakesan.pdf. Accessed 22 December 2015

Jolly AD, Thompson G, Norton GE (2002) Locating pyroclastic flows on Soufriere Hills Volcano, Montserrat, West Indies, using amplitude signals from high dynamic range instruments. J Volcanol Geotherm Res 118:99–317. doi:10.1016/S0377-0273(02)00299-8

Kaneko T, Maeno F, Nakada S (2014) Ontake 2014 eruption: observation from a helicopter. Proceedings of the 2014 Fall Meeting of the Volcanological society of Japan, Fukuoka, Japan, 2-4 November 2014. (In Japanese)

Kato A, Terakawa T, Yamanaka Y, Maeda Y, Horikawa S, Matsuhiro K, Okuda T (2015) Preparatory and precursory processes leading up to the 2014 phreatic eruption of Mount Ontake, Japan. Earth Planets Space 67:111. doi:10.1186/s40623-015-0288-x

Kawase H, Matsuo H (2004) Separation of source, path, and site effects based on the observed data by K-NET, KiK-net, and JMA Strong motion network. J Jpn Assoc Earthq Eng 4(1):33–52. doi:10.5610/jaee.4.33 (In Japanese with English abstract)

Kobayashi T (1980) The 1979 eruption of Ontake volcano. In: Aoki H (ed) Investigation of volcanic activity and disasters caused by the 1979 eruption of Ontake volcano. Nagoya University, Nagoya, pp 4–12 (In Japanese)

Koyanagi S, Aki K, Biswas N, Maeda K (1995) Inferred attenuation from site EFFECT-corrected T phase recorded on the island of Hawaii. Pure Appl Geophys 144:1–17. doi:10.1007/BF00876471

Kumagai H, Nakano M, Maeda T, Yepes H, Palacios P, Ruiz M, Arrais S, Vaca M, Molina I, Yamashina T (2010) Broadband seismic monitoring of active volcanoes using deterministic and stochastic approaches. J Geophys Res 115:B08303. doi:10.1029/2009JB006889

Kumagai H, Placios P, Ruiz M, Yepes H, Kozono T (2011) Ascending seismic source during an explosive eruption at Tungurahua volcano, Ecuador. Geophys Res Lett 38:L01306. doi:10.1029/2010GL045944

Kumagai H, Lacson R Jr, Maeda Y, Figueroa MS II, Yamashina T, Ruize M, Palacios P, Ortiz H, Yepes H (2013) Source amplitudes of volcano-seismic signals determined by the amplitude source location method as a quantitative measure of event size. J Volcanol Geotherm Res 257:57–71. doi:10.1016/j.jvolgeores.2013.03.002

Leonard GS, Stewart C, Wilson TM, Procter JN, Scott BJ, Keys HJ, Jolly GE, Wardman JB, Cronin SJ, McBride SK (2014) Integrating multidisciplinary science, modelling and impact data into evolving, syn-event volcanic hazard mapping and communication: A case study from the 2012 Tongariro eruption crisis, New Zealand. J Volcanol Geotherm Res 286:208-232. doi: 10.1016/j.jvolgeores.2014.08.018.

Maeda Y, Kato A, Terakawa T, Yamanaka Y, Horikawa S, Matsuhiro K, Okuda T (2015) Source mechanism of a VLP event immediately before the 2014 eruption of Mt. Ontake, Japan. Earth Planets Space 67:187. doi:10.1186/s40623-015-0358-0

Matsumoto Weather Station (1991) Volcanic activity of Ontakesan. Report of Coordinating Committee for Prediction of Volcanic Eruption 50:10–12 (In Japanese)

Nagano Prefectural Government (2015) Information about the eruption of Ontake volcano on September 27, http://www.pref.nagano.lg.jp/bosai/kurashi/shobo/saigai/260927ontake.html. Accessed 22 December 2015. (In Japanese)

Nagoya University (1991) Volcanic activity of Ontakesan from April to May, 1991. Report of Coordinating Committee for Prediction of Volcanic Eruption 50:13–15 (In Japanese)

Nakamichi H, Kumagai H, Nakano M, Okubo M, Kimata F, Ito Y, Obara K (2009) Source mechanism of a very-long-period event at Ontake volcano, central Japan: response of a hydrothermal system to magma intrusion beneath the summit. J Volcanol Geotherm Res 187(3-4):167–177. doi:10.1016/j.jvolgeores.2009.09.006

Ogiso M, Yomogida K (2012) Migration of tremor locations before the 2008 eruption of Meakandake Volcano, Hokkaido, Japan. J Volcanol Geotherm Res 217–218:8–20. doi:10.1016/j.jvolgeores.2011.12.005

Otsuka Y, Fujimatsu J (2009) Identification of volcanic earthquakes at Ontake volcano. Q J Seismol 72:85–90 (In Japanese)

Phillips WS, Aki K (1986) Site amplification of coda waves from local earthquakes in central California. Bull Seismo Soc Am 76(3):627–648

Taisne B, Brenguier F, Shapiro NM, Ferrazzini V (2011) Imaging the dynamics of magma propagation using radiated seismic intensity. Geophys Res Lett 38:L04304. doi:10.1029/2010GL046068

Takagi A, Kitagawa S, Miyamura J (2007) Crustal deformation around Ontake volcano detected by GPS observation. In: Proceedings of the Japan Geoscience Union Meeting, Chiba, Japan, 19-24 May 2007.

Takagi A, Yamamoto T, Yokoyama H, Nakahashi M, Kato K (2014) Tilt change and shallow pressure source associated with the 2014 Ontakesan eruption. In: Proceedings of the 2014 Fall Meeting of the Volcanological society of Japan, Fukuoka, Japan, 2-4 November 2014 (In Japanese)

Takarada S, Oikawa T, Furukawa R, Hoshizumi H, Geshi N, Itoh J, Miyagi I (2014) Estimation of eruptive total mass of the Sep. 27, 2014 Ontake phreatic eruption. In: Proceedings of the 2014 Fall Meeting of the Volcanological society of Japan, Fukuoka, Japan, 2-4 November 2014 (In Japanese)

Takemura S, Furumura T, Saito T (2009) Distortion of the apparent S-wave radiation pattern in the high-frequency wavefield: Tottori-Ken Seibu, Japan earthquake of 2000. Geophys J Int 178:950–961. doi:10.1111/j.1365-246X.2009.04210.x

Tokyo Volcano Observation and Information Center (2014) Annual Volcanic Activity Report (2014), http://www.data.jma.go.jp/svd/vois/data/tokyo/STOCK/monthly_v-act_doc/tokyo/2014y/312_14y.pdf. Accessed 22 December 2015. (In Japanese)

Wessel P, Smith WHF (1998) New, improved version of the Generic Mapping tools released. EOS Trans AGU 79:579

Yamamoto M, Sato H (2010) Multiple scattering and mode conversion revealed by an active seismic experiment at Asama volcano, Japan. J Geophys Res 115:B07304. doi:10.1029/2009JB007109

Yamaoka K (2015) Remaining problem in the national and local government action against the volcanic hazards. In: Proceedings of the Japan Geoscience Union Meeting, Chiba, Japan, 24-28 May 2015.

Yamasato H (1997) Quantitative analysis of pyroclastic flows using infrasonic and seismic data at Unzen volcano, Japan. J Phys Earth 45:397–416. doi:10.4294/jpe1952.45.397